Entropy **2013**, *15*, 5362-5383; doi:10.3390/e15125362

OPEN ACCESS

entropy

ISSN 1099-4300

www.mdpi.com/journal/entropy

Article

Ribozyme Activity of RNA Nonenzymatically Polymerized from 3′,5′-Cyclic GMP

Samanta Pino [1], Giovanna Costanzo [2], Alessandra Giorgi [3], Jiří Šponer[4], Judit E. Šponer [4] and Ernesto Di Mauro [1,*]

[1] Fondazione "Istituto Pasteur-Fondazione Cenci-Bolognetti" c/o Dipartimento di Biologia e Biotecnologie "Charles Darwin", "Sapienza" Università di Roma, P.le Aldo Moro, 5, Rome 00185, Italy; E-Mail: samantapino78@libero.it

[2] Istituto di Biologia e Patologia Molecolari, CNR, P.le Aldo Moro, 5, Rome 00185, Italy; E-Mail: giovanna.costanzo@uniroma1.it

[3] Dipartimento di Scienze Biochimiche, "Sapienza" Università di Roma, P.le Aldo Moro, 5, Rome 00185, Italy; E-Mail: alessandra.giorgi@uniroma1.it

[4] Institute of Biophysics, Academy of Sciences of the Czech Republic, Královopolská 135, Brno 61265, Czech Republic; CEITEC-Central European Institute of Technology, Masaryk University, Campus Bohunice, Kamenice 5, Brno CZ-62500, Czech Republic; E-Mails: jiri.sponer@ceitec.muni.cz (J.S.); judit@ncbr.muni.cz (J.E.S.)

* Author to whom correspondence should be addressed; E-Mail: ernesto.dimauro@uniroma1.it; Tel.: +39-0649-912-880; Fax: +39-0644-408-12.

Received: 13 September 2013; in revised form: 19 November 2013 / Accepted: 22 November 2013 / Published: 3 December 2013

Abstract: 3′,5′-Cyclic GMP spontaneously nonenzymatically polymerizes in a base-catalyzed reaction affording G oligonucleotides. When reacted with fully or partially sequence-complementary RNA (oligo C), the abiotically generated oligo G RNA displays a typical ribozyme activity consisting of terminal ligation accompanied by cleavage of an internal phosphate site of the donor oligonucleotide stem upon attack of the acceptor 3′ terminal OH. This reaction is dubbed Ligation following Intermolecular Cleavage (LIC). In a prebiotic perspective, the ability of oligo G polynucleotides to react with other sequences outlines a simple and possible evolutionary scenario based on the autocatalytic properties of RNA.

Keywords: RNA; RNA polymerization; RNA origin; ribozymes; origin of life

---

1. Introduction

In the quest for the initial (pre)genetic materials, the autocatalytic potential of RNA [1–6] remains unmatched. RNA provides, for the time being, the only plausible solution to self-generation, as allowed by self-polymerization and by a variety of self-catalytic processes. Pioneering reports of RNA recombination have appeared [7–12]. With the possible exception of the systems described in [13–15], the reactions reported so far are not simple and robust enough to be of likely prebiotic relevance.

The dissolution of cyclic purine nucleotides (markedly of 3′,5′-cGMP) in water results in the formation of oligonucleotides by their spontaneous nonenzymatic polymerization [16,17]. The reaction is low yielding, but nevertheless, it shows that, although inefficient, RNA may generate itself from prebiotic precursors [18–20]. The conditions for self-polymerization of cyclic pyrimidine nucleotides have not been determined, yet. Early pioneering approaches are reviewed in [21–23]. Efficient enzyme-free copying of all four pre-activated nucleobases, templated by immobilized RNA, was reported [24].

The ligation of preformed RNA oligonucleotides by nonenzymatic ligation was also observed [25–27]. In spite of its low efficiency, this quasi-isoenergetic reaction highlights a mechanism potentially entailing generation of chemical heterogeneity and complexity. Chain elongation occurs by ligation of both homogeneous [25,27] and heterogeneous [26] sequences.

In vitro generated RNA chains undergo a synthesis/degradation equilibrium limiting the possibility of obtaining, by these reactions alone, molecules which are long and complex enough to be of (pre)biological worth. The kinetics of RNA hydrolysis has been a matter of detailed analyses since the 20s of the past century [28]. An entry to the recent literature is given in [21]. In particular, the physical-chemical conditions were reported in which the 3′O-P bond, the more reactive and less stable chain-bond in RNA, has a longer half-life in polymers than in monomers [29].

Self-cleaving and splicing of RNA exemplify a catalytic process in which the folded structure of RNA mediates a reaction on another part of itself [1–6]. Similar reactions may occur in which the two reactive moieties are not part of the same molecule and come together based on sequence-complementarity or on other structural features. Both involve well established in-line attack of an endogenous or exogenous nucleophile on the phosphorus [3].

Here we report a reaction carried out by nonenzymatically generated oligoG RNAs when challenged with a base-pair complementary sequence. This reaction is dubbed LIC: Ligation following Intermolecular Cleavage. The two complementary sequences ligate and self-cleave. In the cleavage reaction, the 3′OH extremity of each sequence behaves (in ribozyme terminology) [30] as an "acceptor". In the same terminology "donor" refers to the phosphate donor site. This reaction suggests to the existence of a recombination mechanism between complementary sequences resulting in RNA chain elongation by addition at the 3′ extremity in simple RNAs.

From a prebiotic perspective, it is noteworthy that this reaction occurs, as shown here, by the action of spontaneously generated polymers derived from abiotically plausible precursors, enhancing the information content of a polymeric mixture. This mechanism potentially represents a plausible means to generate RNA sequence complexity and to approach the question: how could the extremely complex ribosomal machinery [31] start to evolve and how did the initial RNA transfer functions [32] come about?

2. Experimental

2.1. Materials

2.1.1. Oligonucleotides

Oligonucleotides were purchased from Dharmacon *(*Lafayette, CO, USA*)* and were provided unphosphorylated, at both the 5′ and 3′ Extremities: 5′ GGGGGGGGGGGGGGGGGGGGGGGG 3′, dubbed for brevity G24, and, using the same abbreviation: AG24, A2G24, A3G24, G23A, G23U, G23C, G9, C24, C23G, C23A, C23U, C18A6, C12A12, C6A18, A24, A12U12, A12C12, U24. Here, the sequences express the non-phosphorylated forms. The 5′ and/or 3′ phosphorylated forms are specified where appropriate.

2.1.2. Enzymes

T4 Polynucleotide Kinase (PNK) (EC 2.7.1.78) from England BioLabs (Ipswich, MA, USA; # M0201L) catalyzes the transfer and exchange of P_i from the γ-position of ATP to the 5′-hydroxyl terminus of polynucleotides, and the removal of 3′-phosphoryl group from 3′-phosphoryl polynucleotides. One unit is defined as the amount of enzyme catalyzing the production of 1 nmol of phosphate to the 5′-OH end of an oligonucleotide from [γ-^{32}P]ATP in 30 min at 37 °C.

2.1.3. Ribonucleases

Ribonuclease A (RNaseA) (EC 3.1.27.5) from bovine pancreas catalyzes the cleavage of the P-O 5′ bond of RNA at the 3′ side of a pyrimidine nucleotide leaving a phosphate group connected at 3′, similarly to what occurs in the water-based hydrolytic reaction. RNaseA is specific for 3′-5′ bonds yielding a 2′,3′ cyclic phosphodiester [33,34]. It was purchased from Sigma (St. Louis, MO, USA; catalog no. ENO531-10 MG), assay in H_2O at 98 °C, pH 6.2. One unit of the enzyme causes an increase in absorbance of 1.0 at 260 nm when yeast RNA is hydrolyzed at 37 °C and pH 5.0. Shrimp Alkaline Phosphatase (SAP) (orthophosphoric-monoester phosphohydrolase) (EC 232-631-4) from Promega (Fitchburg, WI, USA, catalog no. M8201) removes phosphate groups from the 5′ position of RNA. One unit will hydrolyze 1 μmole of 4-nitrophenyl phosphate/minute at pH 9.8 at 37 °C.

2.2. Methods

2.2.1. Polymerization of 3′,5′-cyclic GMP

Polymerization of 3′,5′-cyclic GMP was performed as described in the literature [16,17]. In particular, the protocol detailed in [17] was followed. Briefly, guanosine 3′,5′-cyclic monophosphate (3′,5′-cGMP) (Sigma Aldrich, St. Louis, MO, USA; acid form, ca # G7504) was dissolved in MilliQ water at 20 mM concentration, reacted for 60 min at 80 °C in the presence of 10 mM 1,8-diazabicycloundec-7-ene (DBU, Sigma Aldrich). Note that the Na form of 3′,5′-cGMP (Sigma Aldrich, cat # G6129) does not polymerize [17]. The product of polymerization was 5′ end-labelled as described below, typically at 1500 cpm/pmol.

2.2.2. Terminal Labelling of the Material Polymerized from Cyclic Nucleotides

The products of the polymerization reactions from cyclic nucleotides were precipitated with EtOH and dissolved in water. The standard procedure involves a 5′-dephosphorylation step and phosphorylation by kinase and ^{32}PγATP. For dephosphorylation, 1 μL of Shrimp Alkaline Phosphatase (SAP, 1 U/μL) was added along with 5 μL of 10× buffer (1× = 0.05 M Tris-HCl pH 9.8, 10 mM $MgCl_2$). The reaction was incubated at 37 °C for 30 min, phenol extracted and precipitated with EtOH. Glycogen (1 μL of 20 mg/mL stock) was added to facilitate precipitation. The RNA was recovered by centrifugation, dissolved in 16 μL of water and labelled at the 5′-termini with ^{32}P. Phosphorylation was carried out by adding 1 μL of T4 Polynucleotide kinase (PNK: 10 U/μL, New England Biolabs), 2 μL of 10 × PNK buffer and 0.5 μL [γ-^{32}P]ATP, followed by incubation at 37 °C for 30 min. After labelling the oligonucleotides, both those of commercial origin (Dharmacon) and those polymerized from 3′,5′-cGMP, were purified by precipitation. The same results were obtained with oligonucleotides purified from PAGE by band cutting and extraction.

2.2.3. The Ligation Following Intermolecular Cleavage (LIC)

The reaction of the indicated oligonucleotides was performed at the concentrations indicated where appropriate. Typically, 2 pmoles of a 5′γ^{32}P labelled oligonucleotides (typically 1500 cpm/pmol) were reacted in 15 μL (0.13 μM) at 60 °C for 30 min in water with the indicated amount of an unlabelled fully or partially complementary sequence. The reaction was stopped by precipitation, the sample was resuspended in pure formamide, heated at 65 °C for 10 min and analyzed by denaturing PAGE, as detailed [17].

2.3. MALDI-ToF Mass Spectrometry

The product (100 ng) was mixed (1:1) with an aqueous 3-hydroxypicolinic acid matrix solution (20 mg/mL) and analyzed with an AutoFlex II instrument (Bruker Daltonics, Bremen, Germany), equipped with a 337 nm nitrogen laser and operating in reflector positive mode.

2.4. Computational Details

Computations were carried out at DFT-D2 level of theory using the TPSS density functional [35] combined with the D2 empirical dispersion correction introduced by Grimme [36]. All atoms were described with the TZVP basis set [37,38]. Geometry optimizations were performed without any constraints, *i.e.*, with full relaxation of all parameters. The C-PCM continuum solvent approximation [39,40] (ε = 78.4) along with the atomic radii of Klamt and Schüürmann [41] was used throughout the calculations. Free energy of the optimized geometries was calculated as a sum of the total electronic energy and the thermal correction term to the free energy derived from frequency calculations at 298 K in the harmonic approximation. All computational models considered carried a total charge of −1 and are described in detail in the Results and Discussion part. Computations were performed with the Gaussian09 suite of programs [42].

3. Results and Discussion

3.1. The Experimental Plan

We first report the experimental description of the LIC reaction, as determined in the G24 + C24 system (Figure 1). Detailed characterization follows (Figures 2 and 6). The preliminary study of the reaction on well characterized commercially available material has been necessary because to our knowledge this reaction, albeit conceivable [4], has not been explored before. The presumed mechanism is described in Figures 3–5. We then show (Figure 8) that nonenzymatically generated G oligomers (dubbed "neo-oligoG") efficiently perform the LIC reaction.

Schematically: the LIC reaction is first analyzed in a model system consisting of pre-synthesized G 24mers and C 24mers and variants thereof (Section 3.2). The features of the reactions are then verified and confirmed in a shorter-sequence system (G 9mer) (Figure 7, Section 3.3). The ability of the neo-oligoG to carry out the reaction is then examined and characterized (Section 3.4).

3.2. Detection of the LIC Reaction

In what follows, the notation pG24 indicates phosphorylation of the 5′ OH of the RNA chain (G24) and G24p indicates phosphorylation of the 3′ OH. Further, the notation "•p" represents a ^{32}P-carrying phospate group. For the sequence 5′^{32}P-G24-3′OH, the phosphorylation is at the 5′ end of the sequence (•pG24). For the 3′ end, 5′OH-G24-3′^{32}P is abbreviated G24•p. If two independent sequences are joined, for example the case where bonding has occurred between C24 and ^{32}P-G (•pG) forming 5′OH-C24-3′^{32}PG, the notation is C24•pG.

3.2.1. Interaction of Sequence-Complementary Oligonucleotides (G24 + C24) Results in the Production of a New Molecular Species

G 24mer oligonucleotides were reacted with C 24mers. Two different experimental routes were followed. *Route* 1: reaction of 5′ phosphorylated G24 (dubbed in short •pG24) with unphosphorylated C24, and *Route* 2: reaction of 5′ phosphorylated C24 (•pC24) with unphosphorylated G24.

- Route 1: 5′^{32}P-G24-3′OH (•pG24) + 5′OH-C24-3′OH (C24)

Figure 1 shows the results of route (1). •pG24 (2 pmoles in 15 μL = 0.13 μM) was reacted (30 min, 60 °C in water pH 6.0) with increasing amounts of unphosphorylated C24, from 1.5×10^{-2} pmoles in 15 μL (=1×10^{-3} μM. Lane 1) to 3×10^{3} pmoles (200 μM. Lane 19), covering five orders of magnitude of mass ratios between the two oligomers. C24-G24 dimers form which are indicated by **c** (left, top-down lettering). In these reaction conditions part of these dimers are covalently ligated, as previously reported [26] and as quantified in Supplementary Item #1. The sequence complementarity does not imply that the two strands are fully in register and fully coupled. Actually the broad gel regions occupied by input materials (Figure 1A) indicate the contrary (see also Figure 1C).

Figure 1. The reaction of 5′^{32}P-G24 (•pG24) with C24 generates a new molecular combination. Panel A. 2 pmoles of •pG24 were reacted (60 °C, 30 min in 15 μL of water pH 6.0 = 0.13 μM) with increasing amounts of unlabeled C24, from 1×10^{-3} (lane 1) to 2×10^{2} μM (lane 19). The separate leftmost lane U (=Untreated) shows the starting •pG24 material. Lane M is the size marker C24, shown here as 5′ ^{32}P labelled molecule but used in the reaction as unphosphorylated form. The reactions were stopped by precipitation and analyzed in denaturing (8 M urea) 16% acrylamide gels. The •pG24 oligonucleotide (indicated by **a**, top-down lettering) hybridizes with the complementary C24 sequence, yielding the 48mer **c**. Part of the •pG24/C24 hybrid undergoes terminal ligation [26]. This part of the reaction is complete at 1×10^{-2} μM C24 (lane 4). At 2×10^{-2} μM (lane 5) a terminal recombination product C24•pG (**d**) starts to form. Panel B. High resolution denaturing PAGE of •pG24 + C24 (0.13 and 3 μM, respectively). Panel C. Interaction of •pC24 with G24 (route 2). The assay was run as the one described in Panel A. In this case the constructs are in the opposite orientation. 0.13 μM •pC24 was reacted with the indicated amounts of G24. The lower efficiency of formation of species **d** relative to the opposite orientation is evident (see Discussion and Table 1).

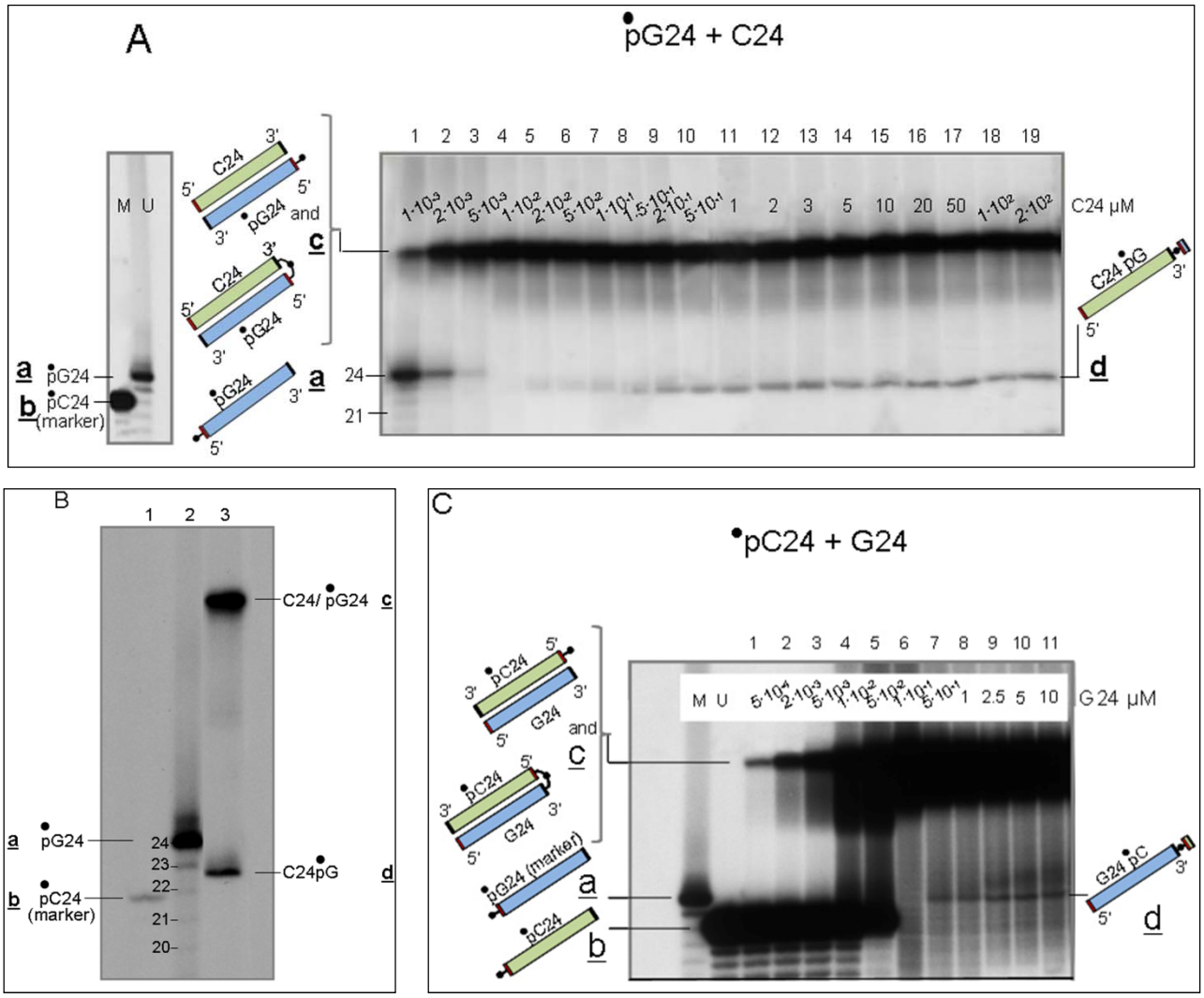

In the Figure, **a** indicates the unreacted •pG24. Upon dissolution in water, oligoGs undergo hydrolysis resulting in a mixture of full-length molecules and shorter fragments. RNA fragments generated by hydrolysis have a 3′ extremity carrying a 2′,3′ cyclic phosphate which is gradually open to yield 2′ or 3′ phosphate extremities [43,44]. As observed by MALDI ToF analysis (see Supplementary Item #2), a part of the short oligomers lose their phosphate and have a 3′ OH extremity. Given that the shorter fragments may also take part in the reactions (see below), they are considered as active components in stoichiometric evaluations.

A new molecular species forms upon interaction of G24 and C24, observed when one of the two reactants is phosphorylated at 5′. This species is referred to by **d** (indicated and cartooned in Figure 1A, right). As shown in the following sections, **d** is a C24mer where, at the 3′ end, a 5′^{32}P-G residue (pG) has been transferred by the LIC reaction.

Figure 1B reports a high-resolution gel showing that when •pG24 [0.13 μM, = species **a**] (lane 2) is reacted (lane 3) with unphosphorylated unlabeled C24 (3 μM) it affords two types of molecules (lane 3): a 48mer (C24/pG24) (**c**) and C24 pG (**d**). Lane 1 shows the position of •pC24 in this gel. [Note that the reaction described is carried on with unphosphorylated C24 and that the ^{32}P labelled sample in lane 1 has the purpose of a position marker.] The position of **d** is 1 nucleotide step higher than the position of pC24, which is coherent with the product expected from the reaction, as depicted in Figure 3. The resulting C24•pG product was characterized enzymatically by RNaseA (Figure 2, panels A and B) and by SAP (Shrimp Alkaline Phosphatase) (Figure 2, panels C and D) analyses of the products of this reaction.

- Route 2: pC24 + G24

A similar behaviour was observed with the mirror-wise combination of oligomers (route 2: pC24 + G24). The results of the reaction of this combination are shown in Figure 1C. Species **d** did form also in this orientation, although in lower amounts (see Table 1 and Discussion).

3.2.2. Characterization of Molecules **d**, Product of Reaction LIC

Molecules **d** are (i) composed of cytosines and, at the 3′end, carrying (ii) a ^{32}P-labelled phosphate group followed by a guanosine residue, as determined by evidence shown below:

(i) Evidence that **d** is almost entirely made of cytosines is provided by specific RNaseA analyses (Figure 2). Given that the C24 oligomer is introduced in the assay as unphosphorylated unlabeled molecule, the acquired phosphate is necessarily derived from the 5′ ^{32}P labelled G24 oligomer (•pG24).

(ii) The 3′ position of the acquired phosphate group is established by 5′ specific exonuclease (Shrimp Alkaline Phosphatase) treatment (Figure 2C,D). Validation of this result is provided by an hybridization competition assay (Supplementary Item #3).

Figure 2. RNaseA and Shrimp Alkaline Phosphatase analyses of the products of •pG24 + C24 reaction. RNaseA. Panel A: •pG24 (0.13 μM) (right marker, lane M) was reacted with C24 (1 μM) in water in standard conditions (as in Figure 1), then adjusted to 20 μL and treated at 98 °C (see Methods) with 0, 0.005, 0.05, 0.5, 5, 50 units of RNaseA (lanes 1–6, respectively). The left marker lane M shows the position of •pC24.Panel B: plot of the residual amount of the **c** and **d** species, as indicated (% relative to the initial amount, lane 1) as a function of the increasing RNaseA units. Shrimp Alkaline Phosphatase. Panel C: •pG24 (0.13 μM) (lane 1) was reacted in 20 μl of SAP buffer (see Methods) with 5 SAP Units for 0, 30, 60 and 180 min (lanes 1–4). •pG24 (0.13 μM) was reacted with C24 (1 μM) (30 min, 60 °C) and similarly treated for 0, 30, 60 and 180 min (lanes 5–8). Panel D: plot of the residual amount of the **a**, **c** and **d** components, as indicated (% relative to the initial amounts, lane 4), as a function of increasing reaction time.

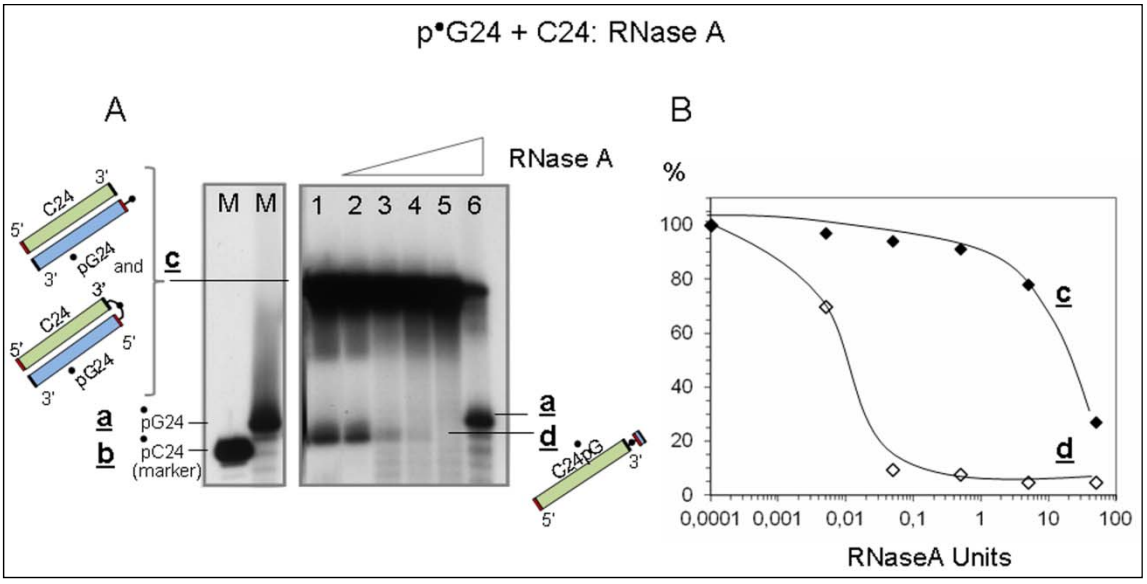

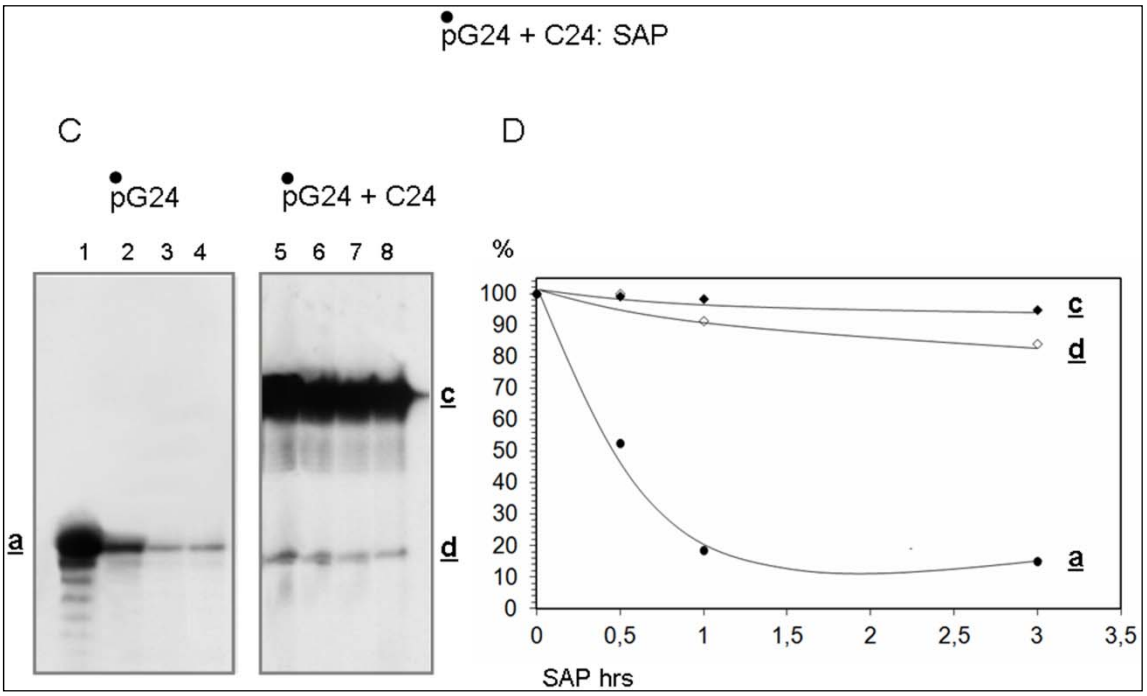

3.2.3. Determination of the Position of the ^{32}P-labelled Phosphate Group

Ribonuclease A

RNaseA catalyzes the cleavage of the P-O$^{5'}$ bond of RNA at the 3′ side of a pyrimidine nucleotide leaving a phosphate group connected at the 3′-end. This property allows the determination of the sequence composition of species **d**.

The products of the reaction of •pG24 with C24 were analyzed. Namely, RNaseA treatment was performed on a sample containing the •pG24/C24 48mer **c** and the C24•pG **d**. The sample was obtained by reaction of 0.13 μM of •pG24 with 1 μM C24 (similar to sample 11 in Figure 1A) and was treated with increasing concentrations of RNaseA, as indicated in the legend (Figure 2A). The gel image and the plot (panel B) show that the C24•pG species **d** is very sensitive to RNaseA. This is expected for a C-containing oligo, each phosphoester bond 3′ of a cytidine nucleotide being target for RNaseA, as outlined in the scheme below pointing to the RNaseA sensitive sites in **d**.

↓ ↓ ↓

d: 5'Cp(Cp)$_{22}$C•pG

In contrast, the C24/•pG24 48mer becomes sensitive only at high RNaseA concentration due to protection of the C-component by the G-strand. At sufficiently high intensity of treatment (lane 6) also the C-moiety of the GC double strand is eventually attacked and the •pG24 component (**a**) is released (lane 6). We have observed that the selectivity for cleavage at 3′ of a pyrimidine residue is conserved till a RNaseA concentration of 0.25 U/μL. Above that concentration also PuPy bonds are attacked (see Supplementary Material in [26]).

The C24•pG species **d** is the most sensitive, which agrees with its single-stranded, free strand structure and pyrimidine composition. In conclusion, the differential sensitivities to RNaseA of the newly formed molecules confirm the proposed structures.

Shrimp Alkaline Phosphatase (SAP)

Is the ^{32}P labelled phosphate group acquired by the C-oligonucleotide in species **d** encompassed into an internal phosphodiester bond or does it bind at the terminal end of sequence exposing the external phosphate? And, if external, is it at 5′ or at 3′?

SAP is an exonuclease that dephosphorylates at 5′ but not at 3′ nor, as secondary activity, at internal sites. This property allows the determination of the position of the ^{32}P-labelled phosphate group on RNA molecules.

The products of the reaction of •pG24 with C24 (obtained as described in Figure 1) were analyzed. Namely, SAP treatment was performed on a sample containing •pG24 (**a**) (left panel), and on a sample (right panel) containing the C24/•pG24 48mer (**c**) and the C24•pG (**d**) of interest. The sample was obtained by reaction of 0.13 μM of •pG24 with 1 μM C24 (similar to sample 11 in Figure 1) and was treated with 5U of SAP for increasing times. Figure 2 panel C shows the digestion pattern of •pG24 **a** (lanes 1–4) and of the reaction products (**c, d**) (lanes 5–8). Panel D quantifies these data. The molecules bearing the ^{32}P phosphate group at 5′ (•pG24 **a**) are sensitive, as expected for RNA

molecules bearing a phosphate group at 5′, while the double-stranded 48mer (**c**) and the C24•pG **d** (bearing the phosphate at 3′) are resistant. In particular, this confirms that **d** bears the ^{32}P phosphate at 3′.

In summary, the newly formed molecular species **d** is (i) sensitive to RNaseA as pyrimidines are; (ii) is one nucleotide longer than the input unphosphorylated unlabeled molecule from which it derives; (iii) has acquired a phosphate group in subterminal 3′ position, as confirmed by SAP analysis. These data are all coherent with the reaction scheme in Figure 3. Other reaction schemes (not detailed) would contradict one or more of these points.

3.2.4. The Ligation Following Intermolecular Cleavage (LIC) Mechanism

The proposed mechanism for the LIC reaction is described in Figures 3, 4 and 5. On the basis of the experimental data Watson-Crick type base complementarity is needed to reach self-cleavage of the interacting oligomers. In order to put the ligation and cleavage reactions into a common frame and fulfill the requirements of Watson-Crick complementarity we conceived a model system in which the two interacting strands are shifted in register by 3–4 bases in the manner shown in Figure 3, enabling the formation of a loop at the 3′-end of the acceptor strand. This loop formation is necessary to bring the 3′-end into an in-line attacking position at the 5′-phosphorylated end of the donor strand (see Figure 3, left). At the same time, it is reasonable to expect that with rather small conformational change the loop can adopt a geometry in which the 5′-phosphorylated end is attacked at the last but one phosphate group (see Figure 3, right).

Figure 3. The ligation following intermolecular cleavage (LIC) mechanism shown in the example of the reaction between C_{24} and 5′-phosphorylated G_{24}. On the left: ligation assuming loop formation at the 3′-end of C_{24} and attack at the phosphorylated 5′-end of G_{24} leading to the formation of $C_{24}G_{24}$. On the right: simultaneous cleavage reaction initiated by the attack of the 3′-end of C_{24} at the last but one phosphate of the 5′-phosphorylated G_{24}. The products of this reaction are $C_{24}G_{23}$ and 5′-phosphorylated guanosine-phosphate, which readily combines with C_{24} leading to the formation of C_{24}pG.

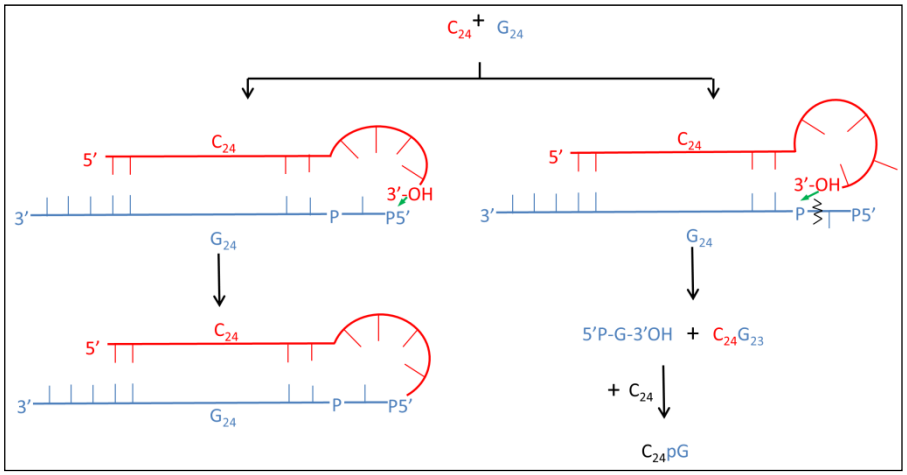

For the theoretical description of the ligation reaction we considered a model (see Scheme 1a) consisting of a donor guanosine-phosphate nucleotide and an acceptor cytidine, which were stabilized by interbase stacking. Three explicit water molecules were added to the phosphate group of the donor

nucleotide in order to provide a more accurate description of the hydration environment of the leaving hydroxyl group. We have computed the free energy profile for the traditional addition-elimination S_N2 scenario of the ligation reaction. The computed free energy profile along with the representative optimized geometries is shown in Figure 4.

Scheme 1. Schematic view of the theoretical models used to describe the ligation (a) and cleavage (b) reactions**.**

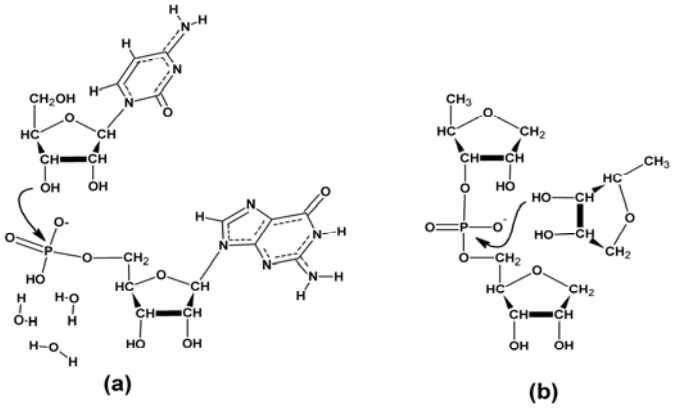

Figure 4. Computed free energy profile of the ligation (orange curve) and cleavage (blue curve) reactions. Computations were carried out at DFT-D2 level of theory. For computational details see Section 2.4.

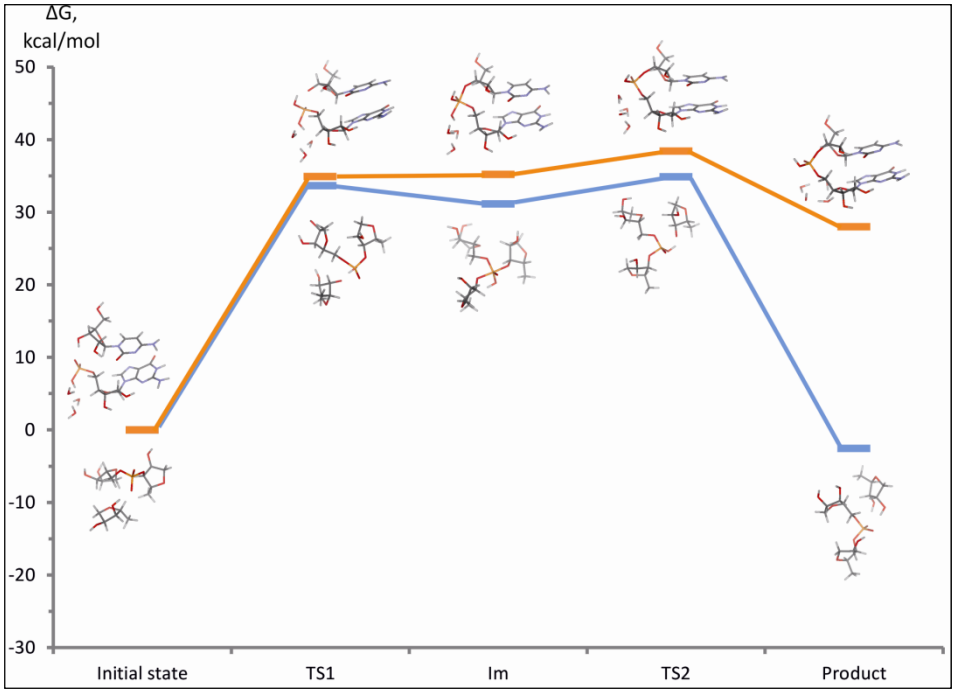

To get an idea about the mechanism of the cleavage of the last but one nucleotide at the 5′-end of the donor strand, first we tried to construct a loop geometry, by altering the dihedrals in a typical double stranded A-RNA geometry in such a way to bring together the ribose of the 3′-end of the acceptor strand and the last but one phosphate of the donor strand to enable an in-line attack (see Figure 5). Since the bases are assumed to not participate directly in the mechanism (see the

segment surrounded with the green curve in Figure 5), in this case our computational model comprised a ribose-phosphate-ribose linkage, which is attacked by another ribose molecule in the manner shown in Scheme 1b. In our computational model both 5′-OH groups were replaced with hydrogens, in order to avoid unphysical H-bond formation between these two groups, which would bias the computations.

Figure 5. Approximate 3D model of a plausible loop geometry that might initiate the cleavage of the 5′-terminal nucleotide of the donor oligonucleotide strand (the direction of the in-line attack is shown with a green arrow, the three nucleotides directly participating in the reaction are surrounded with a green curve).

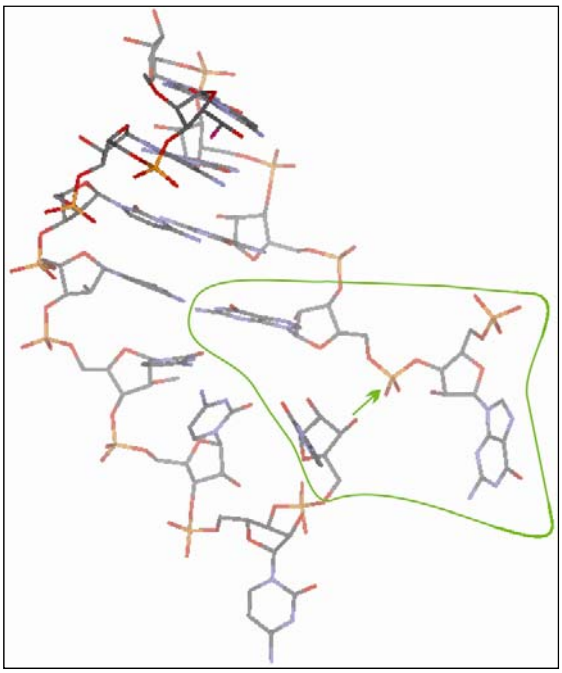

We are aware that the above described two computational models are pretty rough approximations of the experimental reaction complexes. Nonetheless, we think that, in the lack of any structural information, they give a tentative idea about the geometries of the transition states and intermediates of the ligation and cleavage reactions. As for the energetics of the modeled transphosphorylation reactions, similar to other ribozyme mechanisms, this is most likely significantly influenced by delicate structural details that our computational models are unable to account for. On the other hand the free energy profiles shown in Figure 4 unambiguously show that the transphosphorylation mechanism leading to the cleavage of the terminal nucleotide has a very similar (if not better) kinetics as the ligation reaction itself and from the side of thermodynamics it is markedly less endothermic. This also reflects the fact that a hydroxyl group is a much worse leaving group in the case of the ligation reaction than ribose (*i.e.*, nucleotide) involved in the cleavage reaction. The computed reaction free energy change of the cleavage and ligation reactions amounts to −2.6 and 28.0 kcal/mol, respectively. Thus, our calculations suggest that if the loop formation leading to the ligation reaction is feasible then the cleavage of the terminal 5′-phosphorylated nucleotide might take place as well, at least as far as the thermodynamic and kinetic aspects of the reaction are concerned.

The analysis of the product of the LIC reaction requires that C24•pG molecules are released from the Watson-Crick base-paired structures described in Figure 3. The Tm of G-C double-stranded

oligonucleotides was calculated using the Crosslinking Entropy (CLE) Method [45,46]. According to this method the Tm of these molecules at the concentration here used of 1.3 μM is, when fully paired, 86 °C. Thus, the denaturation treatment performed in 100% formamide [47,48] before PAGE analysis ensures strand separation even in fully paired 24mers.

The efficiency of the LIC reaction is low (see below). The titration shown in Figure 1 shows that the maximum yield for LIC is obtained at an acceptor/donor concentration ratio [C24/•pG24] ~ 38.5 (sample 14). Evaluation of the number of C24 molecules that have terminally acquired the •pG group at 3′ (species **d**) was performed measuring the amount of transferred •pG. At plateau, an estimated 10% of the input is transferred. Thus, as range evaluation, 1 molecule of C24•pG is present every *circa* 385 C24 molecules. This might be the consequence of the lower steric accessibility of an internal phosphate group as compared to a chain terminating one in the donor strand. Molecular dynamics simulations addressing this issue are in progress.

3.2.5. Sequence Requirements

How stringent is the structure surrounding the donor site? Figure 6 (panels A and B) shows that generation of species **d** also occurs in the •pG24 + C23A combination (panel A), whose ligation product **c** is C23A•pG24, thus further favouring a bulge in the tip of the ligated molecule. Similar analyses were performed with C23G and C23U (not shown). The plot in Figure 6B shows the relative efficiencies of formation of species **d** with the 4 terminal variants. The maximal LIC yield in the reaction of 0.13 μM •pG24 donor was obtained with 5–20 μM of complementary sequences, the order of efficiency being C > A, G > U, at molar ratios 38.5, 115, 115 and 154 respectively.

The structure of the site surrounding the cleavage point was analyzed in more detail by creation of an increasingly unpaired tip sequence. Figure 6C compares the efficiency of formation of species **d** upon reaction of C24 with •pG24, or •pAG24, or •pA2G24, or •pA3G24. The species **d** produced are indicated by a white asterisk. White dots indicate the untreated 5′ labelled oligonucleotides (U), as indicated on top. In summary, the cleavage pattern shows that the cleavage reaction always occurs at the unpaired tip, even though with less precision (see the multiple bands around the major **d** species), also when the tip contains increasing number of unpaired elements.

Similar results were observed when •pG24 was reacted with other sequences (see Table 1), characterized by different amounts of complementarity (U24, A12U12, A24, A18C6, A12C12, A6C18, C24 and C12A12). In these combinations, the reaction was observed only for C24, A12C12, A6C18 and C12A12, not for U24, A12U12, A24 and A18C6, indicating the requirement of sequence complementarity > 6 nucleotides. This is in line with our mechanistic model shown in Figure 3 right, since formation of a stable loop geometry requires ca. 3–4 WC base pairs, followed by a sequence of 3–4 unpaired bases in the acceptor oligonucleotide strand.

Figure 6. The effects of variations of the ligation sites on the LIC reaction. Variants of the sequence surrounding the ligation site were tested and are shown in panels A through C. Two types of variations are shown: (1) changing the 3′ extremity of the C oligo (C24, C23U, C23G, C23A) (panels A and B); (2) changing the 5′ extremity of the G oligo (•pG24, •pAG24, •pA2G24, •pA3G24) (panel C). All the essays were performed according to the standard protocol: reaction of 0.13 µM of a •p-carrying donor with increasing amounts of fully or partially complementary sequences, as indicated. The plot in panel B shows the amount (%) of species **d** as a function of the acceptor concentration (µM) relative to the maximum amount observed (=100%), for the samples shown in panel A (•pG24/C23A) and for the other not shown samples. In panel C C24 (10 or 100 µM, as indicated) was reacted with the indicated molecules differing for their 5′ extremity. The **d** species is indicated by *.

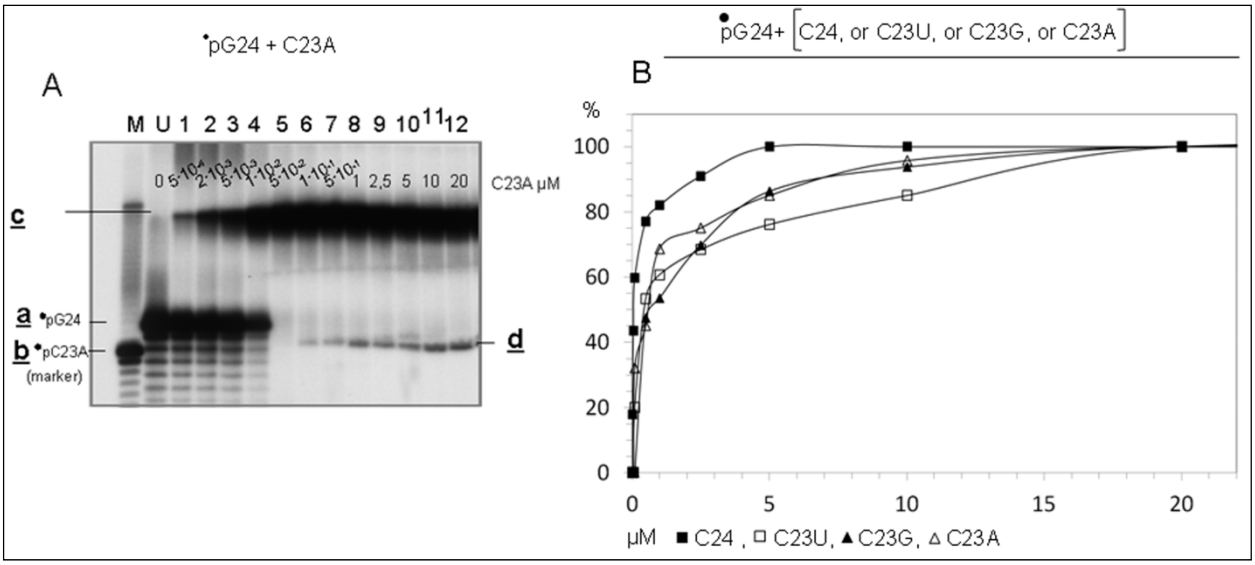

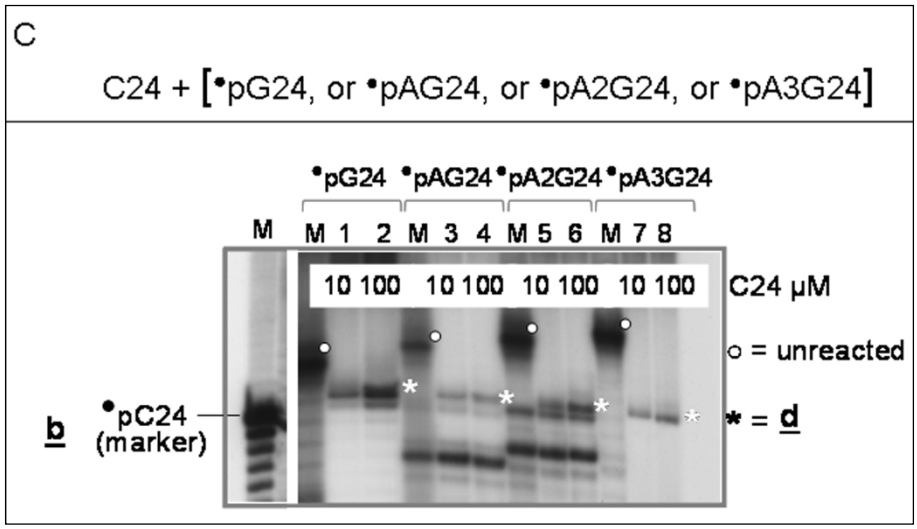

Table 1. The acceptor /donor ratio for the optimal yield of **d** molecule in the LIC reaction.

Construct (A + D)	[A]/[D]	Yield (%)
C24 + •pG24	38.5	10
C23U + •pG24	154	10
C23G + •pG24	115	10
C23A + •pG24	115	10
A12C12 + •pG24	23	5
A6C18 + •pG24	23	5
C12A12 + •pG24	23	5
A24 + •pG24	0	0
U24 + •pG24	0	0
A12U12 + •pG24	0	0
G24 + •pC24	3.8	1
G23U + •pC24	19.2	2
G23A + •pC24	7.7	2
G23C + •pC24	7.7	0.5
C24 + •pG9	7.7	100
C9 + •pG9	7.7	0
C12A12 + •pG9	7.7	100
A12C12 + •pG9	7.7	100
C24 + •p NEO G	4.7	15

The formation of species **d** also occurs in the opposite-orientation combination (•pC24 + G23A), with overall much lower efficiency (data not reported). Similar behaviour was observed with other terminally variant acceptors tested (G23C and G23U). In conclusion, LIC occurs close to the tip of the sequence complementarity-determined structure with not so stringent acceptor sequence requirements.

3.2.6. Complexity

For the overall interpretation of this RNA reaction system, it is important to consider the complexity of the populations of molecules present. In fact, both oligoG and oligoC undergo hydrolysis upon dissolution in water. In the •pG24 case, part of the molecules (up of 85%) generate a population of shorter length, whose 3′ extremity ends with a G residue. Part of these molecules carry at their extremity a phosphate group, part do not and end with an OH (see the MALDI ToF characterization, Supplementary Item #2). Nonetheless, let us stress that product **d** cannot be the product of the ligation reaction between C24 and the hydrolysis product of •pG24, because product **d** is not formed if the donor and acceptor oligonucleotides are too short; *e.g.*, in the reaction of C9 with •pG9 (see Table 1). The overall picture of the population of molecules generated upon dissolution of •pG24 + C24 in water is quite complex. The possibility that ribozyme-like activity is exerted by these shorter molecules has not been explored.

The LIC reaction described above is possibly one of many reactions occurring, identified because of the defined size of the resulting product and because is a "one-step-then-stop" reaction, resulting in a single identifiable product.

3.3. The •pG9 Oligonucleotides also Actively Perform the LIC Reaction

The set of analyses performed with •pG24 was repeated with •pG9 (Figure 7). These analyses were performed because the goal of this study is to explore the possible ribozyme activity of nonenzymatically generated RNAs, which have a major component of short-chained oligo G molecules (see Figure 8). The results confirmed that also •pG9 is an efficient LIC donor for long-chained acceptors with sequence complementarity (C24 and A12C12) and that the corresponding expected species **d** are formed. RNaseA analyses confirmed also in this system the structures and mechanisms described for longer G segments.

Figure 7. •pG9 acts as donor. 0.13 μM of •pG9 reacted in standard conditions with unlabeled unphosphorylated C24 (lane 2, 0.005 μM, lane 3, 1 μM), A12C12 (lane 5, 0.005 μM, lane 6, 1 μM). Lanes 1 and 4 show the corresponding molecules labelled and run alongside as size markers (M). U = unreacted •pG9. The **d** product is indicated (see Text).

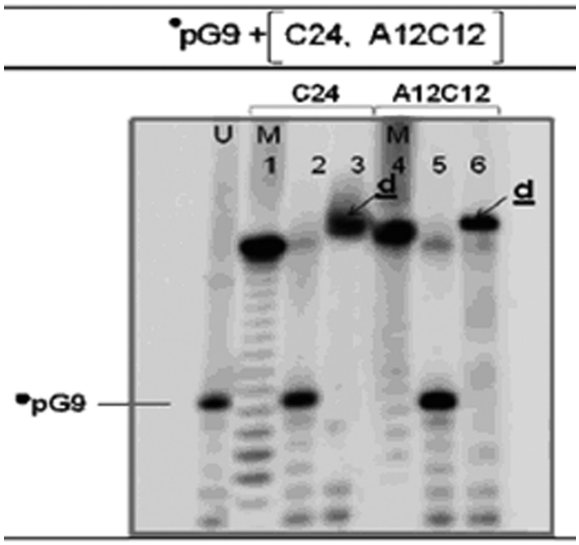

3.4. Spontaneously Polymerized Oligos Perform the LIC Reaction

We have reported [16,17] that 3′,5′-cyclic GMPs nonenzymatically polymerize affording molecules that are 5′ phosphorylated and 3′ OH. Oligomers whose length is centered around 7–8 units prevail, while a subpopulation > 15 nucleotides long slowly forms, reaching a length of 30 nucleotides [16]. The 3′ extremity of the nonenzymatically polymerized polyG RNA generated from 3′,5′-cGMP is unphosphorylated [17].

When reacted with acceptor molecules, also these nonenzymatically polymerized oligonucleotides ("neo-oligoG") perform the LIC reaction. Figure 8 shows that the reaction is efficiently carried out, in agreement with what observed for the synthetic constructs. Panel A shows the reaction of a fixed amount of neo •pG-oligomer (lane 1) with increasing C24 (lanes 2–8). Species **d** forms at high yield. A group of molecules is prominent, which are collectively dubbed as **e**. These molecules are presumably gel retardation forms of the G oligos interacting by base-pairing with the increasing amounts of oligo C.

Figure 8. The LIC reaction performed by nonenzymatically polymerized 3′,5′-cyclic GMP. Panel A: 2.25 pmoles of polymerization products of 3′,5′-cGMP (see Methods) were ^{32}P labeled and run on denaturing PAGE without further treatment (lane 1), or reacted with the indicated increasing amounts of C24. The molarity of the neo •pG oligomers in this assay is 0.15 μM. The formation of species **d** is indicated**.** The star (top right) indicates the neo •pG oligomers bound to the 3′ end of C24 (as detailed in [26]). Panel B: reaction of increasing amounts of neo-•pG oligomers (at the μM indicated on top) reacted with a fixed amount (1 μM) of C24. Panel C: formation of species **d** (% relative to the observed maximum, lane 6) as a function of increasing amount of neo •pG oligomers. Panel D: RNaseA characterization of the products of the interaction of neo-•pG oligomers with C24. Left marker lane: •p C24 marker. Right marker lane: neo •pG oligomer. 0.15 μM neo •pG oligomer was reacted in 20 μL with 1.3 μM C24 (lane 1) in the absence or in the presence of 0.005, 0.05, 0.1, 0.5, 5 and 50 U of RNase A (lanes 2–7), as in Figure 2A. One distorted lane between lanes 2 and 3 was removed.

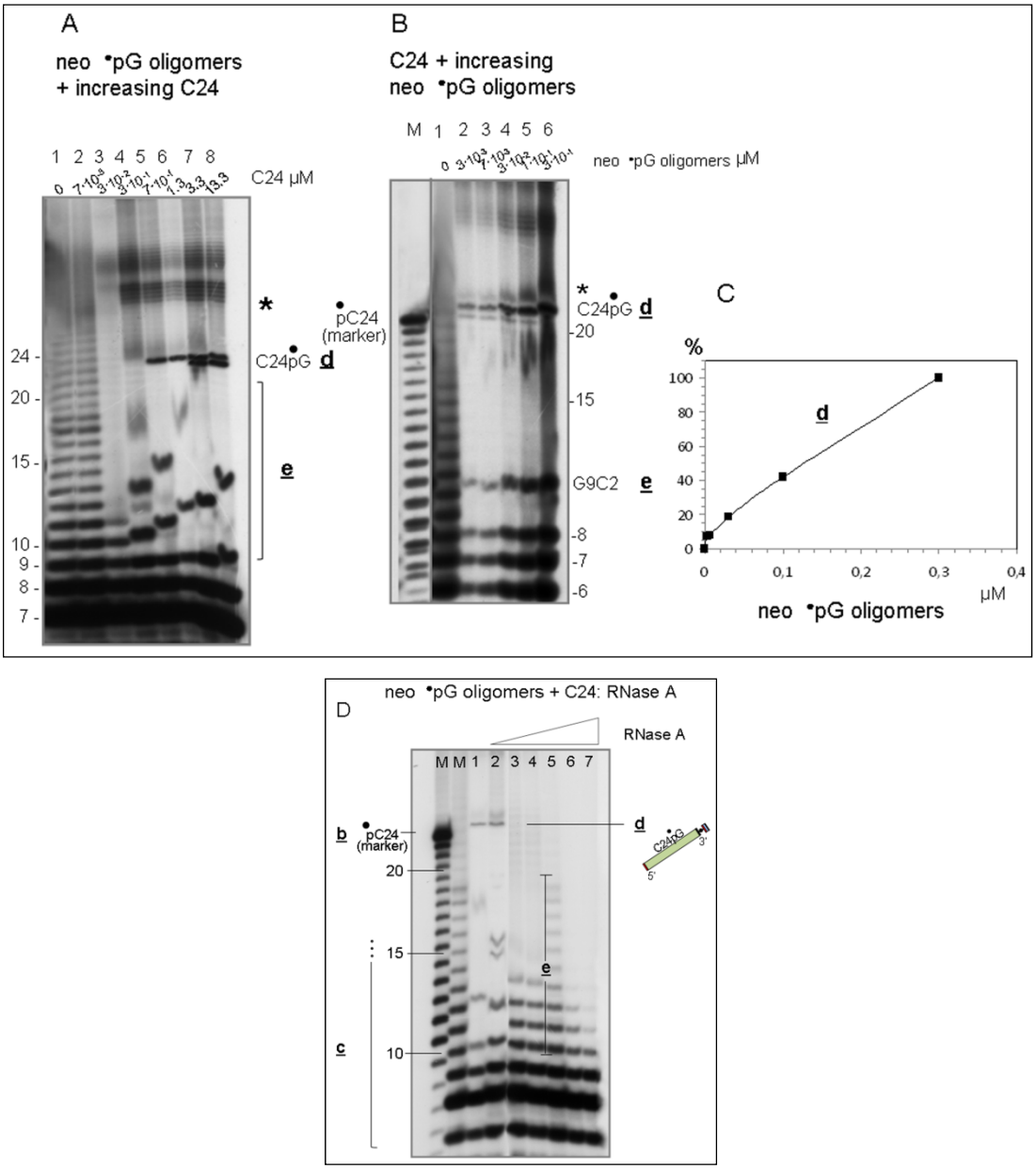

Panel B shows the complementary approach: reaction of a fixed amount of acceptor C24 (1 μM) with increasing neo •pG-oligomer (from 3×10^{-3} to 3×10^{-1} μM). In these conditions C24 is in excess, thus showing that the production of species **d** increases as a function of the increasing phosphate donor sites (Lane 1). The plot in panel C shows that the production of **d** is a linear function of the D/A ratio. This observation unambiguously shows that the intermolecular cleavage is the rate determining step.

The characterization by RNaseA of the reaction product of •p neo G oligomers with C24 is shown in panel D. A sample similar to that shown in Panel A, lane 6 (obtained by reacting 0.15 μM •p neo G oligomers with 1.3 μM C24) was treated with the indicated increasing amounts of RNase A (lanes 2–7). The results (upper panel) show that the species **d** produced by interaction of the nonenzymatically polymerized oligoG with the complementary oligo, behaves exactly as the preformed C24 does: the **d** species (=oligo C + 1G) is highly sensitive and is completely degraded at the low concentration of 0.05 U/assay (0.0025 U/μL, lane 3). The lower part of the panel shows that •pG7, 8, 9 treated in the same conditions in the same reactions are fully resistant. In conclusion, poly G oligomers non-enzymatically polymerized from 3′,5′-cyclic GMP efficiently perform the LIC reaction, exactly as preformed oligomers do.

3.5. Discussion and Evolutionary Implications

The studied RNA molecules deriving from the interactions of nonenzymatically polymerized oligoG with oligonucleotides containing a sufficiently long complementary sequence are active ribozymes. We describe an activity consisting of the nucleophilic attack of an acceptor 3′-hydroxyl group on the phosphorus of a donor 3′,5′ phosphodiester bond. The location of the donor phosphate, the orientation and the structure of the surrounding sequences determine the result consisting of a single cleavage leading to a one-step chain-elongation event.

The cleavage by the 3′ OH of the acceptor molecules preferentially occurs on a XpX step located one step 3′ distal from the 5′ extremity, in unpaired structure, at the tip of the presumptive sequence complementarity-determined double-stranded structure (Figure 3), presumably because the unpaired tip conformation allows local sterical availability. Changing the nature of the tip by insertion of increasing long stretches of A residues at the potential interaction site did not modify the cleavage position.

Thus, in all the analyzed instances the donor site is the XpX step at the first unpaired position at the extremity of a double stranded RNA. This also explains the preference for a single cleavage site. Nevertheless, minor amounts of double or triple cleavages were occasionally observed (Figures 6 and 8).

The acceptor site may be modified and, in the best characterized G donor/C acceptor system (Figure 1A), the structural relationship may be reversed (Figure 1C). However, as calculated from the amount of cleaved molecules produced in the two systems (*i.e.*, •pG24 + C24 *vs.* •pC24 + G24), this latter combination is 10fold less efficient. The acceptor/donor (A/D) ratio for the optimal yield of **d** molecules in the LIC reaction for the various sequence combinations tested is given in Table 1.

In conclusion, transfer of a 5′-terminal G- or C-residue is obtained on the 3′-extremity of the acceptor RNA fragment with various efficiencies, depending on the sequence combination at A/D ratios (best value) encompassed between 3.8 and 154, the % of recombined molecules being encompassed between 0 and 100.

The high acceptor/donor ratio necessary for the reaction indicates that the structural features of the reacting molecules are not optimized. Nevertheless, the fact that the interaction between simple-sequence oligonucleotides leads to further transformation of the sequence information provides the proof-of-principle that the nonenzymatic generation of oligoG RNA molecules from the prebiotically plausible 3′,5′-cyclic nucleotides is the first step of a potentially (pre)genetic process. Interestingly, nor pure polyA nor pure polyU exhibited the type of ribozyme activities reported here.

The prebiotic evolutionary interest of the G:C system was pointed out [49,50]. The reconstruction of molecular events leading to emergence of the triplet code [49,50] suggests that the first genes were formed on the basis of expanding (GCC)*(GGC)n duplexes. The consecutive transesterifications described in the *Tetrahymena* pre-rRNA and cyclization of the excised IVS [3] are a series of chemically homogeneous reactions guided by programmed RNA structures. Three decades of studies of ribozyme activities have revealed the exquisite precision achievable in targeting the reactive sites. Based on the principle that complexity evolved from simplicity, a reasonable guess was proposed [30] for the origin of splice site. According to this reconstruction the proto cleavage site was a GpG step, as resulting from the combination of the donor and acceptor frequency matrices into a single set consisting of 3543 sequences, representing the "average" pattern. The evolution from such a simple system to the extant "three elements" mechanism has been outlined [30,51]. However, no matter how complex the variety of extant ribozyme activities are, they necessarily evolved from initially simple sequences [52,53] endowed with the appropriate chemical potentiality. The data reported here suggest that the properties of the G sequence might have been instrumental in this process.

3.6. Future Plans

We plan to apply additional means to characterize and identify the composition and structure of the products obtained in this study. The limiting factor being the low yield of the products of the LIC reaction, this reaction is, in particular, being characterized on shorter sequences whose efficiency appears to be higher (preliminary results; see also Section 3.4). Synthetic oligonucleotides of different sources will also be analyzed.

Acknowledgments

Thanks to Silvia Lopizzo for helpful contributions. FUNDING: This work was supported by International Firb: RBIN06E9Z8_003. Financial support from the project "CEITEC—Central European Institute of Technology" (CZ.1.05/1.1.00/02.0068) from the European Regional Development Fund and form the Grant Agency of the Czech Republic (Grant No. P208/10/2302) is gratefully acknowledged.

Conflicts of Interest

The authors declare no conflict of interest.

References

1. Guerrier-Takada, C.; Gardiner, K.; Marsh, T.; Pace, N.; Altman, S. The RNA moiety of ribonuclease P is the catalytic subunit of the enzyme. *Cell* **1983**, *35*, 849–857.
2. Zaug, A.J.; Grabowski, P.J.; Cech, T.R. Autocatalytic cyclization of an excised intervening sequence RNA is a cleavage-ligation reaction. *Nature* **1983**, *301*, 578–583.
3. Cech, T.R. The chemistry of self-splicing RNA and RNA enzymes. *Science* **1987**, *236*, 1532–1539.
4. Zaug, A.J.; Cech, T.R. The intervening sequence RNA of Tetrahymena is an enzyme. *Science* **1996**, *231*, 470–475.
5. Doherty, E.A.; Doudna, J.A. Ribozyme structures and mechanisms. *Annu. Rev. Biochem*. **2000**, *69*, 597–615.
6. De Rose, V.J. Two decades of RNA catalysis. *Chem. Biol.* **2002**, *9*, 961–969.
7. Chetverin, A.B.; Chetverina, H.V.; Demidenko, A.A.; Ugarov, V.I. Nonhomologous RNA recombination in a cell-free system: Evidence for a transesterification mechanism guided by secondary structure. *Cell*. **1997**, *88*, 503–513.
8. Chetverin, A.B. The puzzle of RNA recombination. *FEBS Lett.* **1999**, *460*, 1–5.
9. Chetverina, H.V.; Demidenko, A.A.; Ugarov, V.I.; Chetverin, A.B. Spontaneous rearrangements in RNA sequences. *FEBS Lett*. **1999**, *450*, 89–94.
10. Figlerowicz, M.; Bibiłło, A. RNA motifs mediating *in vivo* site-specific nonhomologous recombination in (+) RNA virus enforce *in vitro* nonhomologous crossovers with HIV-1 reverse transcriptase. *RNA* **2000**, *6*, 339–351.
11. Chetverin, A.B. Replicable and recombinogenic RNAs. *FEBS Lett.* **2004**, *567*, 35–41.
12. Chetverin, A.B.; Kopein, D.S.; Chetverina, H.V.; Demidenko, A.A.; Ugarov, V.I. Viral RNA-directed RNA polymerases use diverse mechanisms to promote recombination between RNA molecules. *J. Biol. Chem*. **2005**, *280*, 8748–8755.
13. Striggles, J.C.; Martin, M.B.; Schmidt, F.J. Frequency of RNA-RNA interaction in a model of the RNA World. *RNA*, **2006**, *12*, 353–359.
14. Lutay, A.V.; Zenkova, M.A.; Vlassov, V.V. Nonenzymatic recombination of RNA: Possible mechanism for the formation of novel sequences. *Chem. Biodivers*. **2007**, *4*, 762–767.
15. Obermayer, B.; Krammer, H.; Braun, D.; Gerland, U. Emergence of information transmission in a prebiotic RNA reactor. *Phys. Rev. Lett.* **2011**, *107*, 018101.
16. Costanzo, G.; Pino, S.; Ciciriello, F.; Di Mauro, E. Generation of long RNA chains in water. *J. Biol. Chem.* **2009**, *284*, 33206–33216.
17. Costanzo, G.; Saladino, R.; Botta, G.; Giorgi, A.; Scipioni, A.; Pino, S.; Di Mauro, E. Generation of RNA molecules by base catalyzed click-like reaction. *ChemBioChem* **2012**, *13*, 999–1008.
18. Saladino, R.; Crestini, C.; Neri, V.; Ciciriello, F.; Costanzo, G.; Di Mauro, E. Origin of informational polymers: The concurrent roles of formamide and phosphates. *ChemBioChem* **2006**, *7*, 1707–1714.
19. Costanzo, G.; Saladino, R.; Crestini C.; Ciciriello, F.; Di Mauro, E. Formamide as main building block in the origin of life. *BMC Evol. Biol*. **2007**, *7*, doi:10.1186/1471-2148-7-S2-S1.
20. Costanzo, G.; Saladino, R.; Crestini, C.; Ciciriello, F.; Di Mauro, E. Nucleoside phosphorylation by phosphate minerals. *J. Biol. Chem*. **2007**, *282*, 16729–16735.

21. Saladino, R.; Botta, G.; Pino, S.; Costanzo, G.; Di Mauro, E. Genetics first or metabolism first? The formamide clue. *Chem. Soc. Rev.* **2012**, *41*, 5526–5565.
22. Saladino, R.; Crestini, C.; Pino, S.; Costanzo, G.; Di Mauro, E. Formamide and the origin of life. *Phys. Life Rev.* **2012**, *9*, 84–104.
23. Benner, S.A.; Kim, H.J.; Cardigan, M.A. Asphalt, water, and the prebiotic synthesis of ribose, ribonucleosides, and RNA. *Accounts Chem. Res*. **2012**, *45*, 2025–2034.
24. Deck, C.; Jauker, M.; Richert, C. Efficient enzyme-free. Copying of all four nucleobases templated by immobi-lized RNA. *Nature Chem.* **2011**, *3*, 603–608.
25. Pino, S.; Ciciriello, F.; Costanzo, G.; Di Mauro, E. Nonenzymatic RNA ligation in water. *J. Biol. Chem.* **2008**, *283*, 36494–36503.
26. Pino, S.; Costanzo, G.; Giorgi, A.; Di Mauro, E. Sequence complementarity-driven nonenzymatic ligation of RNA. *Biochemistry* **2011**, *50*, 2994–3003.
27. Pino, S.; Biasiucci, M.; Scardamaglia, M.; Gigli, G.; Betti, M.G.; Mariani, C.; Di Mauro, E. Nonenzymatic ligation of an RNA oligonucleotide analyzed by atomic force microscopy. *J. Phys. Chem. B* **2011**, *115*, 6296–6303.
28. Levene, P.A.; Jorpes, E. The rate of hydrolysis of ribonucleotides. *J. Biol. Chem.* **1929**, *81*, 575–580.
29. Saladino R.; Crestini, C.; Ciciriello, F.; Di Mauro, E.; Costanzo, G. Origin of informational polymers: differential stability of phosphoester bonds in ribo monomers and oligomers. *J. Biol. Chem.* **2006**, *281*, 5790–5796.
30. Stephens, R.M.; Schneider, T.D. Features of spliceosome evolution and function inferred from an analysis of the information at human splice sites. *J. Mol. Biol.* **1992**, *228*, 1124–1136.
31. Yonath, A. Polar bears, antibiotics, and the evolving ribosome (Nobel Lectures). **2010**, *49*, doi:10.1002/anie.201001297.
32. Turk, R.M.; Chumachenko, N.V.; Yarus, M. Multiple translational products from a five-nucleotide ribozyme. *Proc. Natl. Acad. Sci. USA* **2010**, *107*, 4585–4589.
33. Cuchillo, C.M.; Parés, X.; Guasch, A.; Barman, T.; Travers, F.; Nogués, M.V. The role of 2′,3′-cyclic phosphodiesters in the bovine pancreatic ribonuclease A catalysed cleavage of RNA: Intermediates or products? *FEBS Lett.* **1993**, *333*, 207–210.
34. Raines, R.T. Ribonuclease A. *Chem. Rev*. **1998**, *98*, 1045–1066.
35. Tao, J.M.; Perdew, J.P.; Staroverov, V.N.; Scuseria, G.E. Climbing the density functional ladder: Nonempirical meta-generalized gradient approximation designed for molecules and solids. *Phys. Rev. Lett*. **2003**, *91*, 146401.
36. Grimme, S. Semiempirical GGA-type density functional constructed with a long-range dispersion correction. *J. Comp. Chem*. **2006**, *27*, 1787–1799.
37. Schaefer, A.; Horn, H.; Ahlrichs, R. Fully optimized contracted Gaussian-basis sets for atoms Li to Kr. *J. Chem. Phys*. **1992**, *97*, 2571–2577.
38. Schaefer, A.; Huber, C.; Ahlrichs, R. Fully optimized contracted Gaussian-basis sets of triple zeta valence quality for atoms Li to Kr. *J. Chem. Phys.* **1994**, *100*, 5829–5835.
39. Barone, V.; Cossi, M. Quantum calculation of molecular energies and energy gradients in solution by a conductor solvent model. *J. Phys. Chem. A* **1998**, *102*, 1995–2001.
40. Cossi, M.; Rega, N.; Scalmani, G.; Barone, V. Energies, structures, and electronic properties of molecules in solution with the C-PCM solvation model. *J. Comp. Chem.* **2003**, *24*, 669–681.

41. Klamt, A.; Schüürmann, G. COSMO: A new approach to dielectric screening in solvents with explicit expressions for the screening energy and its gradient. *J. Chem. Soc. Perkin Trans.* **1993**, *2*, 799–805.
42. *Gaussian* 09, Revision, A.1; computer program for electronic structure modeling; Frisch, M.J.; Trucks, G.W.; Schlegel, H.B.; Scuseria, G.E.; Robb, M.A.; Cheeseman, J.R.; Scalmani, G.; Barone, V.; Mennucci, B.; Petersson, G.A. *et al.*; Gaussian, Inc.: Wallingford, CT, USA, 2009.
43. Soukup, G.A.; Breaker, R.R. Relationship between internucleotide linkage geometry and the stability of RNA. *RNA* **1999**, *5*, 1308–1325.
44. Li, Y.; Breaker, R.R. Kinetics of RNA degradation by specific base catalysis of transesterification involving the 2′-hydroxyl group. *J. Am. Chem. Soc*. **1999**, *121*, 5364–5372.
45. Dawson, W.; Yamamoto, K.; Kawai, G. A new entropy model for RNA: Part I. A critique of the standard Jacobson-Stockmayer model applied to multiple cross links. *J. Nucleic Acids Investig*., **2012**, *3*, e3.
46. Dawson, W.; Yamamoto, K.; Shimizu, K.; Kawai, G. A new entropy model for RNA: Part II. Persistence-related entropic contributions to RNA secondary structure free energy calculations. *J. Nucleic Acids Investig.* **2013**, *4*, e2.
47. McConaughy, B.L.; Laird, C.D.; McCarthy, B.J. Nucleic acid reassociation in formamide. *Biochemistry* **1969**, *8*, 3289–3295.
48. Casey, J.; Davidson, N. Rates of formation and thermal stabilities of RNA:DNA and DNA:DNA duplexes at high concentrations of formamide. *Nucleic Acids Res*. **1977**, *4*, 1539–1552.
49. Trifonov, E.N. The triplet code from first principles. *J. Biomol. Struc. Dyn.* **2004**, *22*, 1–11.
50. Rapoport, A.E.; Trifonov, E.N. "Anticipated" Nucleosome positioning pattern in prokaryotes. *Gene* **2011**, *488*, 41–45.
51. Hickey, D.A.; Benkel, B. Introns as relict retrotransposons: Implications for the evolutionary origin of eukaryotic mRNA splicing mechanisms. *J. Theor. Biol.* **1986**, *121*, 283–291.
52. Saladino R.; Crestini, C.; Costanzo, G.; Di Mauro, E. On the Prebiotic Synthesis of Nucleobases, Nucleotides, Oligonucleotides, pre-RNA and pre-DNA Molecules. In *Prebiotic Chemistry;* Walde, P., Ed.; Topics in Current Chemistry; Springer: Berlin, Germany, 2005; Volume 259, pp. 29–68.
53. Cleaves, H.J.; Michalkova Scott, A.; Hill, F.C.; Leszczynski, J.; Sahai, N.; Hazen, R. Mineral-organic interfacial processes: Potential roles in the origins of life. *Chem. Soc. Rev*. **2012**, *41*, 5502–5525.